December 1966

USCEE Report 183

UNIVERSITY OF SOUTHERN CALIFORNIA

SCHOOL OF ENGINEERING

FINAL REPORT

MILLIMETER-WAVE RADIOMETRY FOR RADIO ASTRONOMY

W. V. T. Rusch
S. D. Slobin
C. T. Stelzried

Contract No. JPL 951424

Prepared for

JET PROPULSION LABORATORY
PASADENA, CALIFORNIA

ELECTRONIC SCIENCES LABORATORY

December 1966 USCEE Report 183

MILLIMETER-WAVE RADIOMETRY FOR RADIO ASTRONOMY

W. V. T. Rusch
S. D. Slobin
C. T. Stelzried

FINAL REPORT

Contract No. JPL 951424

This work was performed for the Jet Propulsion Laboratory, California Institute of Technology, sponsored by the National Aeronautics and Space Administration under Contract NAS7-100.

Prepared for

JET PROPULSION LABORATORY
PASADENA, CALIFORNIA

TABLE OF CONTENTS

I. HISTORY OF THE PROGRAM 1

II. INSTRUMENTATION DEVELOPMENT 3

III. ANTENNA DEVELOPMENT 4

A. Feedhorn Redesign 4
B. Nodding Subdish 7
1. Analysis 7
2. Mechanical Construction and Performance 11
3. RF Performance 17

IV. SOLAR OBSERVATIONS 20

V. LUNATION OBSERVATIONS 23

VI. PUBLICATIONS 25

APPENDIX 26

REFERENCES 31

ACKNOWLEDGEMENT 32

I. HISTORY OF THE PROGRAM

In September, 1963, the mm-wave instrumentation program was initiated as a joint effort between the Jet Propulsion Laboratory and the Electrical Engineering Department of the University of Southern California. The JPL participation was conducted through the New Circuit Elements Group of the Communications Elements Research Section, which provided equipment and personnel involved primarily with the electronic instrumentation.

The Electrical Engineering Department contributed the antenna, a converted 60-inch searchlight. Personnel were provided to design the antenna and feed system, the associated drive system, etc. USC personnel also directed the astronomical aspects of observation of the lunar eclipse of 30 December 1963. During the period from September 1963 to July 1964 USC participation was sponsored by a grant from the Research Corporation, Contract AJ4-205 638 from JPL, and financial support for salaries and equipment from the EE Department, Joint Services Grant, AF-AFOSR-495-64.

In August, 1964 a JPL study contract was issued to the USC Electrical Engineering Department (JPL Contract No. 951 004). The purpose of this contract was to investigate and develop high sensitivity MM-wave receivers and the techniques of their application to scientific and technological experimentation. The original contract period was from 1 August 1964 to 31 July 1965; however, a two-month extension changed the termination date to 30 September 1965. A second study contract (JPL Contract No. 951 424) was issued to cover the period from 1 October 1965 to 15 September 1966. This contract continued the previous work as a joint JPL-USC program. The mm-wave radiometer and associated electronic technologies were the primary areas of interest and responsibility of JPL, although there was considerable participation by USC personnel in the design and assembly stages of the radiometer, particularly during the summer months. The chief responsibilities of the USC personnel were antenna design and performance, the scientific observational program, the theoretical analyses, and data reduction. The overall long-range planning of the entire program was a mutual effort.

II. INSTRUMENTATION DEVELOPMENT

Since the system used for lunation measurements during the summer of 1965 (Ref. 1) was close to the ultimate development goals, a great deal of new equipment was not developed during the period covered by this present report. Minor adjustments and updating of existing equipment were carried out to provide an adequate operating system for the lunar and solar observations.

A TRG, Inc. ferrite waveguide switch was installed to replace a deteriorating and well-used existing switch. Similarly, long usage had degraded the output of the Tucor, Inc. gas tube and this was replaced by an ITT, Inc. gas tube. Various combinations of mixer diodes were tried to minimize the receiver noise figure. A new waveguide run was installed to reduce signal loss between the waveguide horn and the mixer.

Following the lunar and solar observations and antenna pattern measurements, it was decided to install a commercially available radiometer "rear-end" in the existing system. This radiometer (AIL type 2392B Universal Radiometer) replaced part of the IF amplifiers, the Princeton, Inc. phase detector, and parts of the DC signal system. The advantages of having a commercial radiometer are ease of servicing, commercial availability of parts, and compatibility with many types of existing instrumentation. Quantitative comparisons will be made between the original system and the AIL Radiometer and will be reported in the next report.

III. ANTENNA DEVELOPMENT

A. Feedhorn Redesign

One component of the original radiometer needing improvement was the antenna feedhorn. Cassegrainian optics are used in the antenna, and the feedhorn illuminates the hyperboloidal subreflector. It is highly desirable that the feedhorn have an axially symmetric pattern, a relatively narrow beam, and low sidelobes to minimize forward spillover. The original feedhorn used in the radiometer was a dual-mode circular horn with a matching iris (Ref. 2). However, in the haste to design this horn for the 1963 eclipse, only a minimum effort was devoted to optimizing the design.

Furthermore, because of the matching iris, the dual-mode configuration is quite narrow band. Currently available 90-Gc klystrons, which are used in the radiometer as a local oscillator, are not well frequency-stabilized. The resulting frequency instability in a narrow-band rf front end leads to degradation of radiometer gain and sensitivity. Consequently, it was felt desirable to incorporate a different feedhorn configuration in the radiometer.

The design selected was the diagonal-horn type (Ref. 3). The horn (shown in Figures 1 and 2) consists of three regions: an E-band waveguide region with flange, a transition region, and a long, tapered region with rotated square cross-section. The completed unit was gold flashed. The measured VSWR was less than 1.05 over a frequency range from 89.60 Gc to 90.30 Gc.

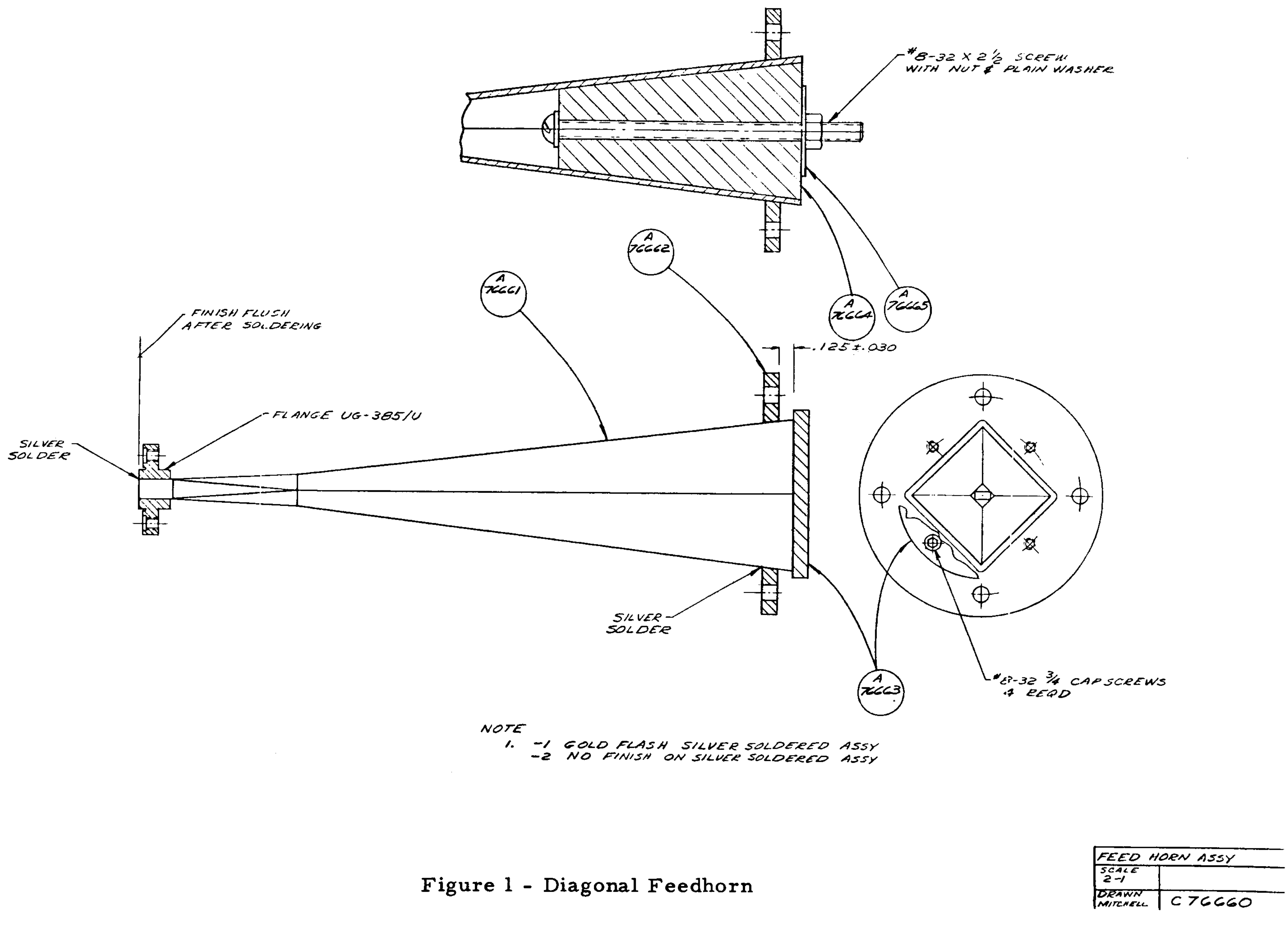

Figure 1 - Diagonal Feedhorn

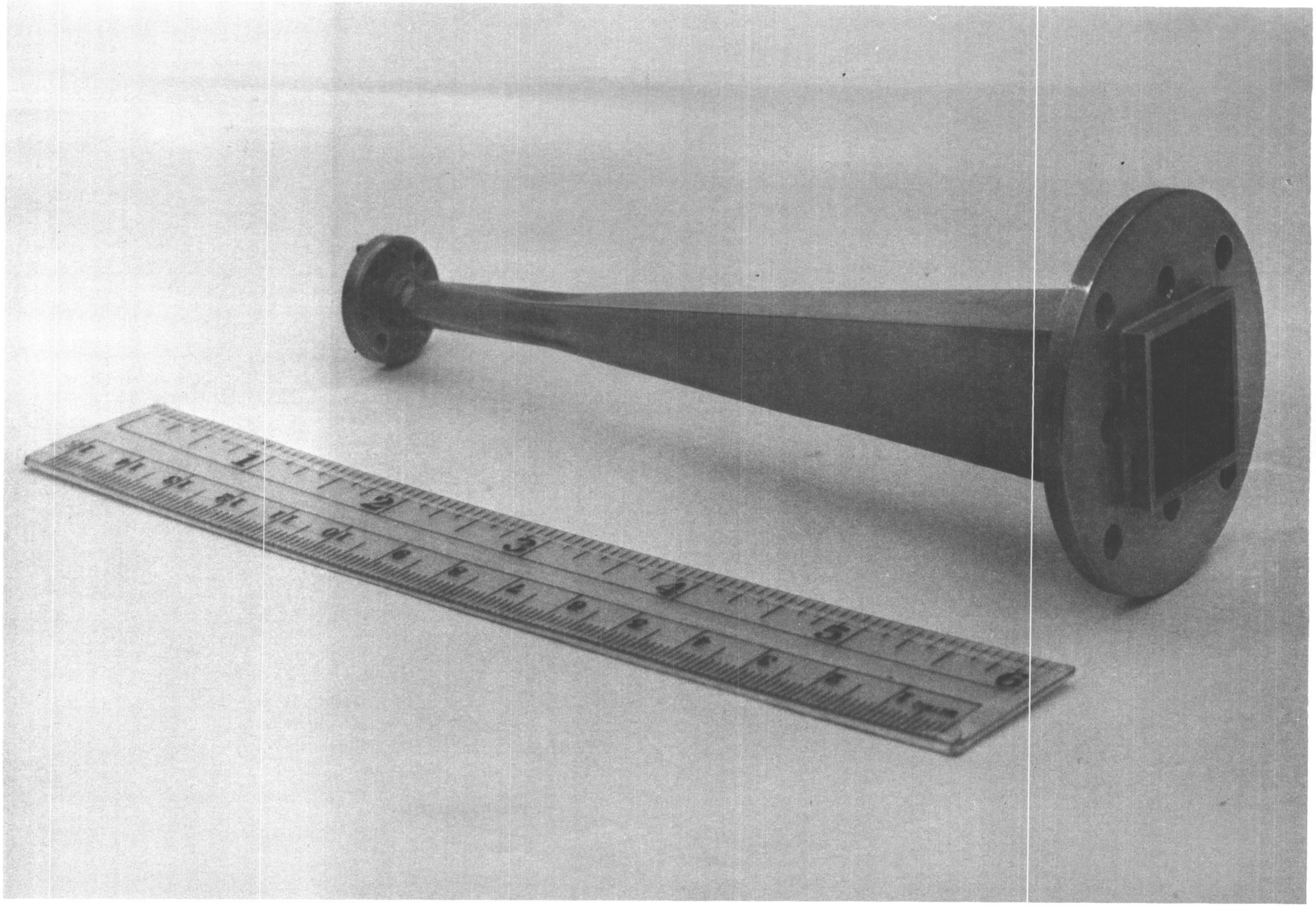

Figure 2 - Diagonal Feedhorn

B. Nodding Subdish

The development of a nodding subdish beam-switching system has been the major project of the contract period. Not only was it necessary to design, fabricate, and test the subdish itself, it was also necessary to carry out a detailed theoretical analysis of the electromagnetic aspects of the problem. A preliminary description of the nodding subdish system may be found in the last final report (Ref. 1).

1. Theoretical Analysis - Scattering from an asymmetric hyperboloid has been solved previously in the literature (Ref. 5) using the techniques of geometrical optics. In order to obtain more accurate expressions for important diffraction effects, the problem of scattering from a tilted hyperboloid was solved using vector diffraction theory. The geometry is shown in Figure 3.

The hyperboloid is axially symmetric in the x_3, z_3 system. The equation for its surface in this system is

$$\rho_3 = \frac{-ep}{1 + e \cos \theta_3} \qquad \text{[Eqn 1]}$$

where

$$p = c\left(1 - \frac{1}{e^2}\right),$$

$$e = \text{eccentricity}, >1$$

$$c = \tfrac{1}{2}\overline{OF}$$

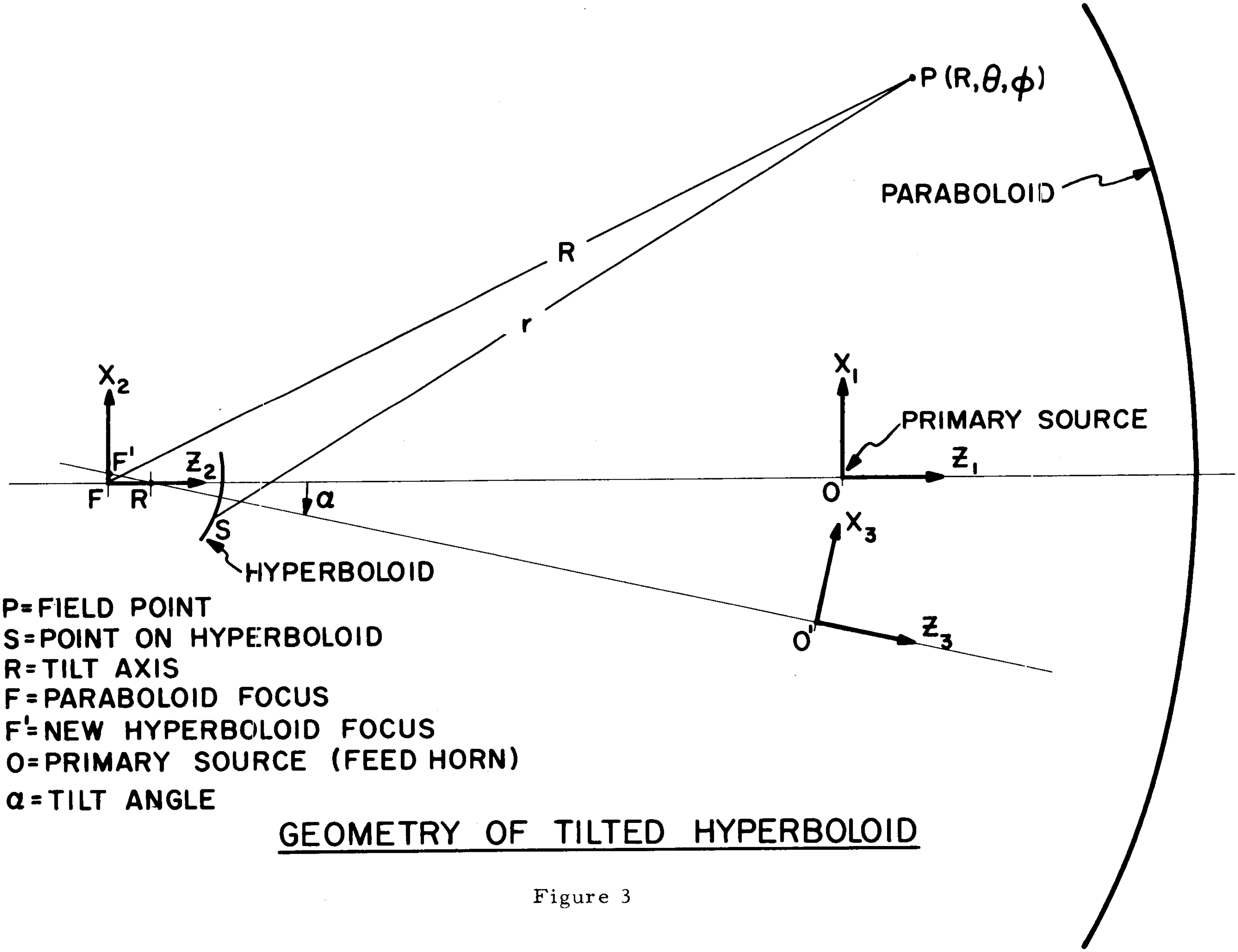

GEOMETRY OF TILTED HYPERBOLOID

Figure 3

The primary field emanates from 0 (in the x_1, z_1 system) in the form of a **spherical** wave and impinges on the hyperboloid. The scattered field at the field point P is (Ref. 4)

$$\overline{E}(P) = \frac{-j\omega\mu}{2\pi} \int [\overline{n} \times \overline{H}_i]_{\text{transverse}} \cdot [\frac{e^{-jkr}}{r}] \, dS \qquad \text{[Eqn 2]}$$

For ease of solution, the integration is carried out in the x_3, z_3 system. However, in order to compute the field scattered from the paraboloid, it is necessary to evaluate the scattered field $\overline{E}(P)$ in the x_2, z_2 system. Thus, three coordinate systems are involved in the problem.

Evaluating factors in the integrand, and performing necessary coordinate transformations, the following multi-coordinate expressions are obtained:

$$E_\theta(P) = \frac{-j(kep)}{2\pi} \frac{e^{-jkR}}{R} \int_{\theta_0}^{\pi} \frac{\sin\theta_3}{(1 + e\cos\theta_3)^2} \cdot$$

$$\cdot \left[\int_0^{2\pi} \frac{\rho_3}{\rho_1} A(\theta_1) M(\theta_3, \varphi_3) e^{-jk\rho_1} e^{jk\rho_2 [\sin\theta \sin\theta_2 \cos(\varphi - \varphi_2) + \cos\theta\cos\theta_2]} d\varphi_3 \right] d\theta_3$$

[Eqn 3]

$$E_\varphi(P) = \frac{-j(kep)}{2\pi} \frac{e^{-jkR}}{R} \int_{\theta_0}^{\pi} \frac{\sin\theta_3}{(1 + e\cos\theta_3)^2} \cdot$$

$$\cdot \left[\int_0^{2\pi} \frac{\rho_3}{\rho_1} A(\theta_1) N(\theta_3, \varphi_3)\, e^{-jk\rho_1} e^{jk\rho_2 [\sin\theta \sin\theta_2 \cos(\varphi - \varphi_2) + \cos\theta \cos\theta_2]} d\varphi_3 \right] d\theta_3$$

[Eqn 4]

where $A(\theta_1)$ = primary source feed function

$M(\theta_3, \varphi_3) = (DH-EG)\cos\theta\cos\varphi + (EF-CH)\cos\theta\sin\varphi + (CG-DF)(-\sin\theta)$

$N(\theta_3, \varphi_3) = (DH-EG)(-\sin\varphi) + (EF-CH)\cos\varphi$

and

$C(\theta_3, \varphi_3) = \cos\alpha(\sin\theta_3 \cos\varphi_3) - \sin\alpha(e + \cos\theta_3)$

$D(\theta_3, \varphi_3) = \sin\theta_3 \sin\varphi_3$

$E(\theta_3, \varphi_3) = \sin\alpha(\sin\theta_3 \cos\varphi_3) + \cos\alpha(e + \cos\theta_3)$

$F(\theta_1, \varphi_1) = (1 + \cos\theta_1)\sin\varphi_1 \quad \cos\varphi_1$

$G(\theta_1, \varphi_1) = \cos\theta_1 \sin^2\varphi_1 - \cos^2\varphi_1$

$H(\theta_1, \varphi_1) = -\sin\theta_1 \sin\varphi_1$

$k\rho_1, k\rho_2, \theta_1, \varphi_1, \theta_2, \varphi_2$ are all related through coordinate transformations to θ_3 and φ_3

$E_\theta(P)$, $E_\varphi(P)$ are referred to the x_2, z_2 coordinate system

Numerical integration of Equations 3 and 4 has been undertaken. The resulting computer program is shown in the Appendix.

2. Mechanical Construction and Performance - The nodding subdish moves between two off-axis positions, symmetric with respect to the centerline of the operating mechanism. The axis about which the dish moves may be indexed to give movement in any desired direction. Provision is also made for focussing the subdish by means of an internal motor, gear drive, and lead screw. Located on the back of the subdish is a small cam follower and two small bearings. Located on the circular counterweight are similar cam follower and similar bearings. The four bearings fit into a holder located in a fixed position with respect to the adjustment plate. The cam followers fit into a two-track cam wheel which is driven by an external motor. All these various parts may be seen in Figures 4 through 10.

Rotation of the cam wheel causes approximate "square-wave" motion of both the subdish and the counterweight. The subdish remains in one off-axis position for about 45% of the rotation of the cam wheel, switches for 5% of the rotation, remains in the second position for 45% of the rotation, and then switches back to the first position during the remaining 5% of the cam wheel rotation.

The nodding subdish mechanism has been set up in a permanent laboratory bench testing apparatus. The mechanism was operated slowly for a short period of time to observe the operation at low speeds (1 to 2 cycles per second). The speed of operation was then increased, and close visual and audio observations were made with regard to resonances, vibrations, possible surface deformation, and cam wear. Although operation was extremely noisy at 8 cps (the maximum tested so far), no mirror surface

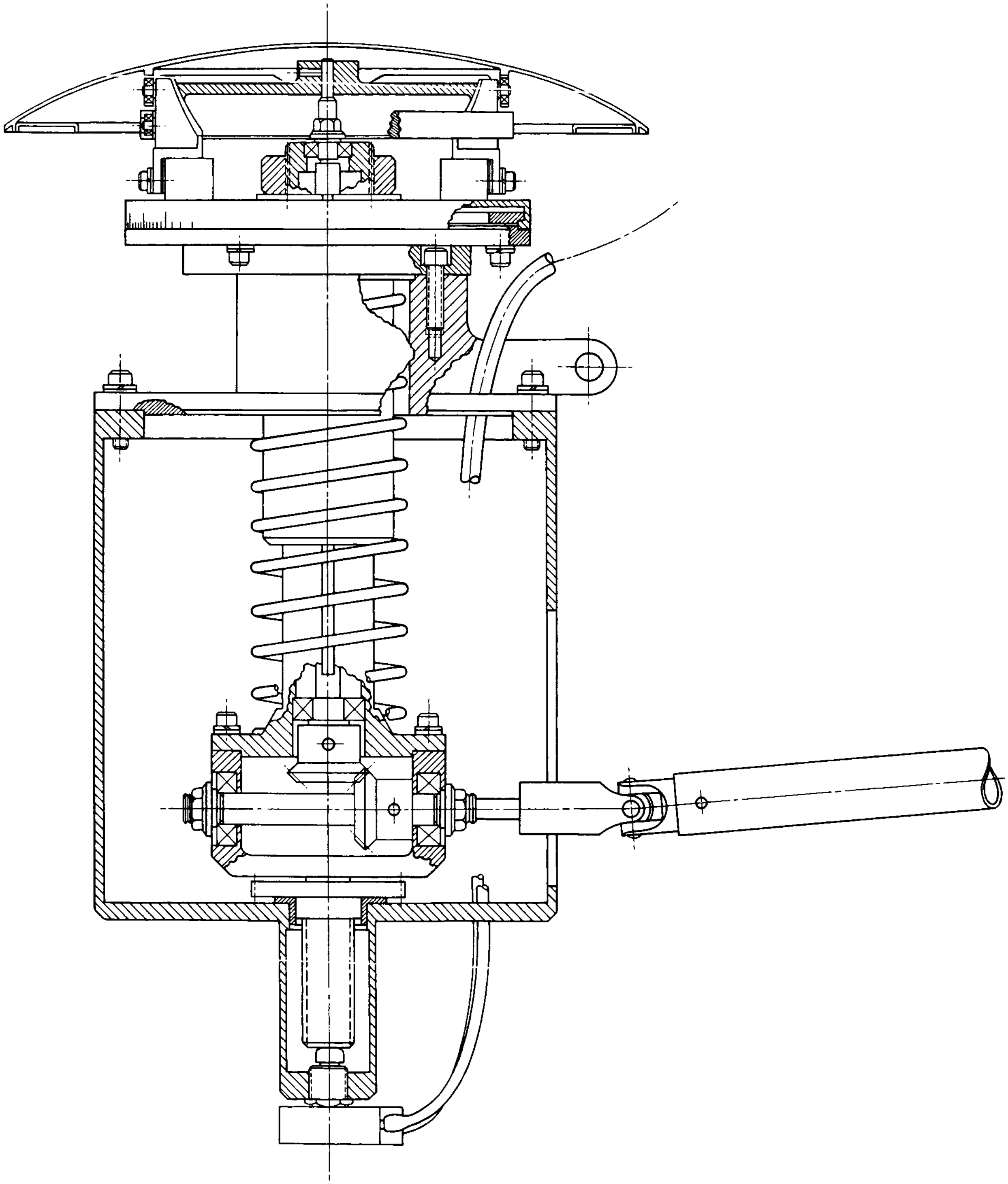

Figure 4 - Hyperbolic Reflector Mount Assembly

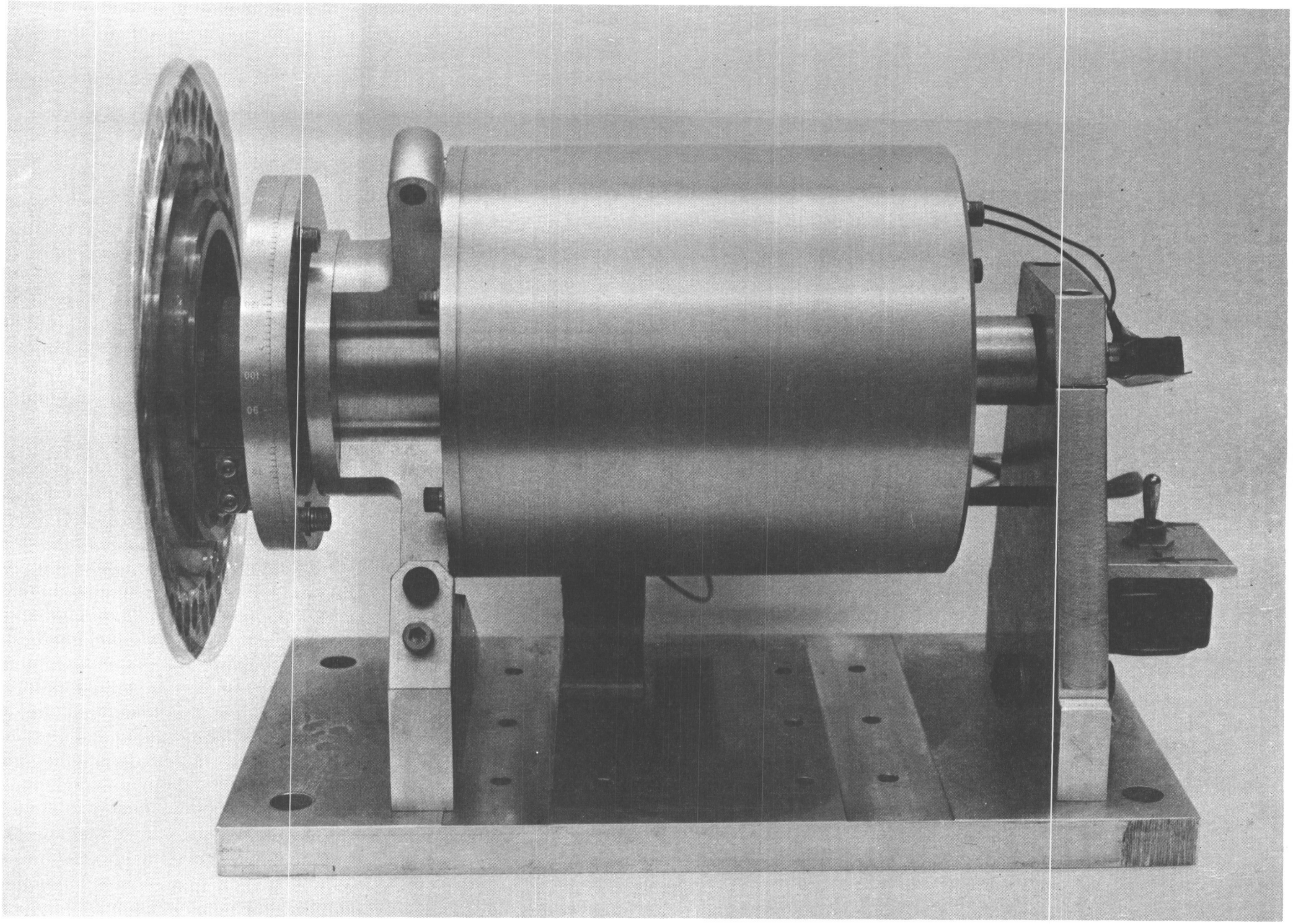

Figure 5 - Side view of nodding subdish assembly showing extremes of mirror motion during switching cycle

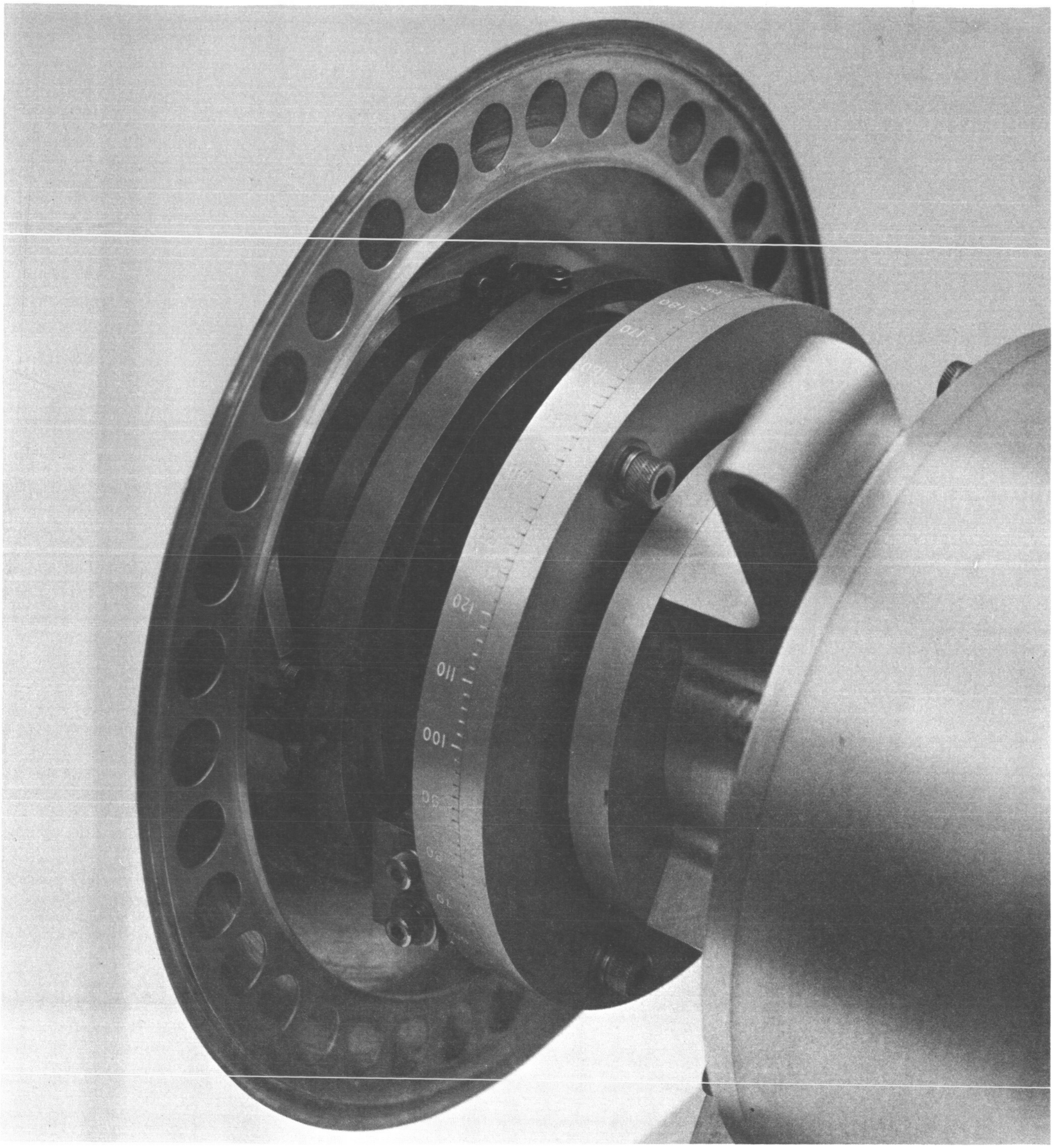

Figure 6 - Back view of subdish assembly showing mirror stiffening ring, bearing holders, cam follower, cam wheel, counterweight, indexing plate, and tripod head

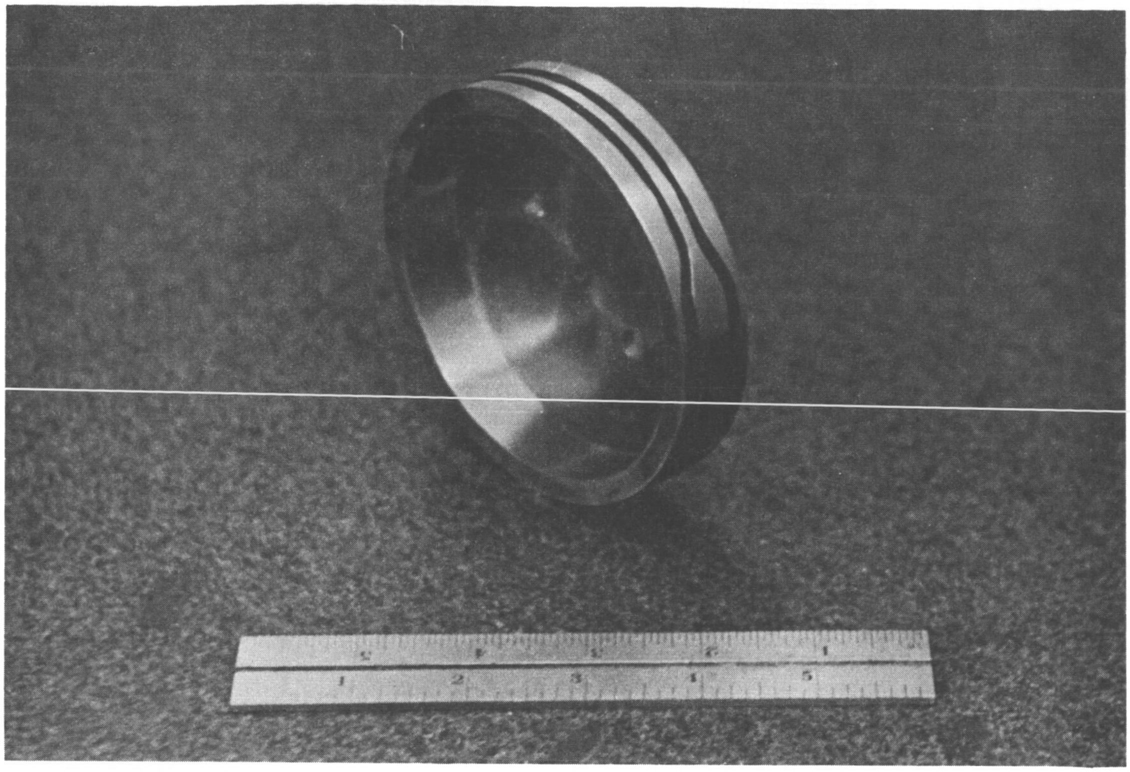

Figure 7 - Cam wheel showing symmetrical cam tracks

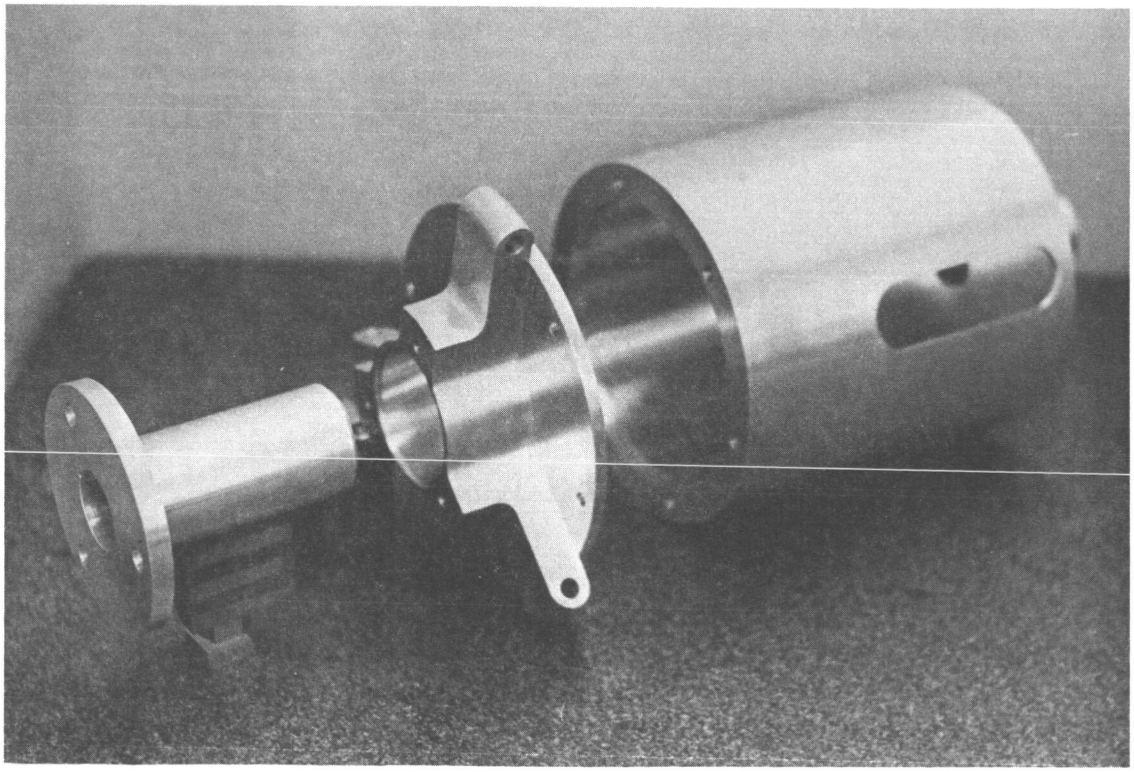

Figure 8 - Exploded view of hyperbolic reflector mount, l. to r.: sleeve for main shaft, tripod head main housing

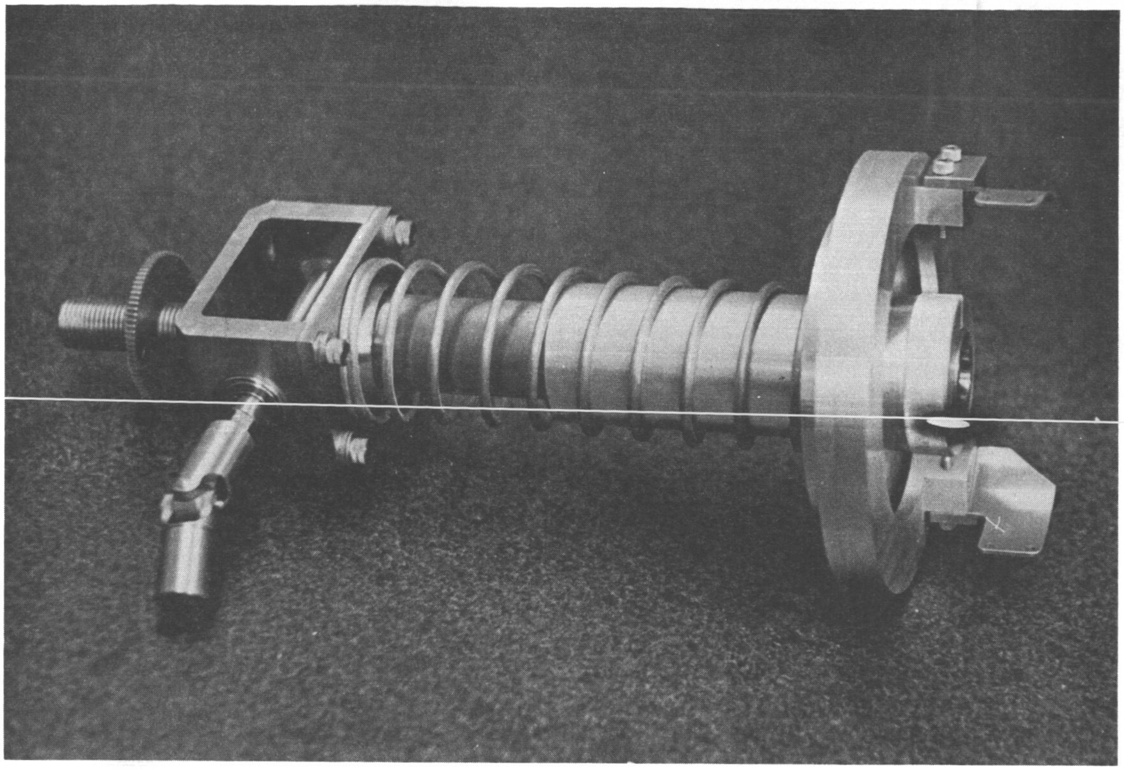

Figure 9 - Focussing and drive unit showing universal joint for external drive, miter gear housing, focussing screw and gear, focussing spring, indexing plate, and bearing holders

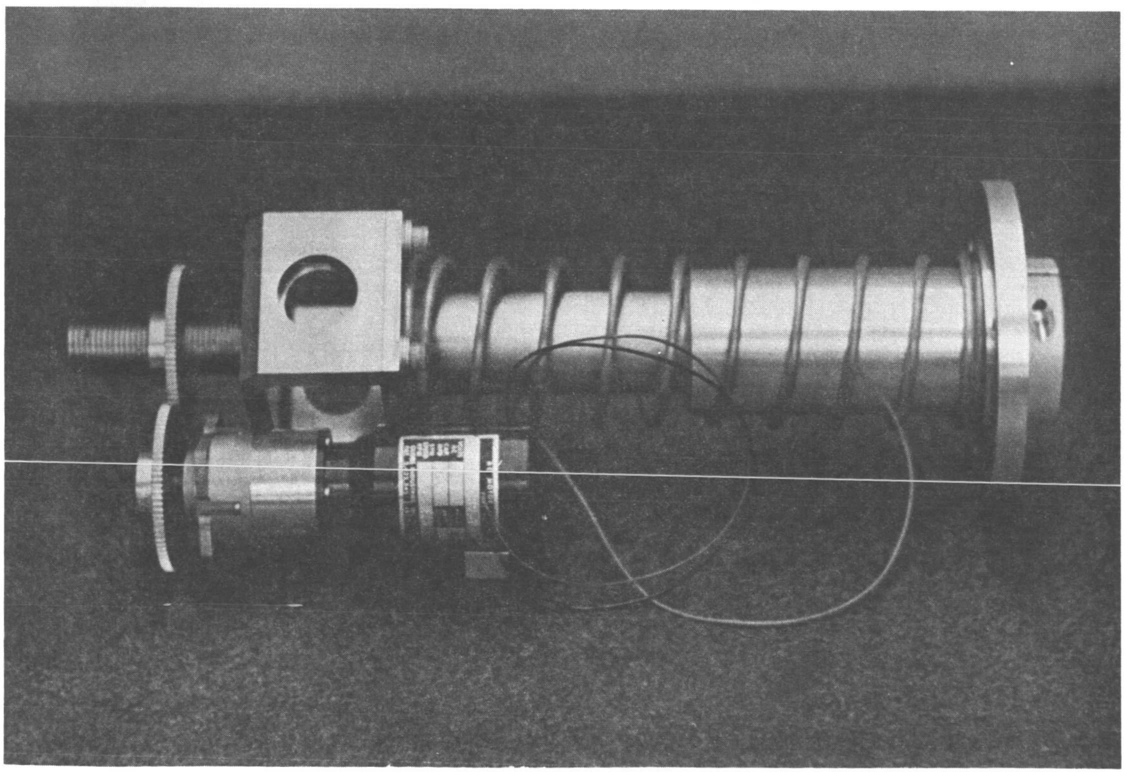

Figure 10 - Focussing unit showing focussing motor, focussing gears and screw, and focussing spring

deformations or cam follower distortions were noted using a strobe light to "freeze" the motion of the mechanism during operation. At the present time it is felt that operation at 6-1/6 cycles per second (a relatively smooth operating point) is possible from both an electronic and mechanical standpoint.

3. RF Performance - Antenna pattern measurements have been taken using the tilted hyperboloid in one stationary position tilted 2° from its symmetric position (axis of hyperboloid colinear with axis of paraboloid). The total excursion from one extreme of tilt to the other is 4°. The total beam shift between extremes is 55.5 minutes of arc. Hence, the deviation of the beam from its symmetric position is 27.75 minutes of arc.

Figures 11 and 12 show the static antenna patterns measured with the subdish tilted to its 2°-off-axis position. Comparison of these patterns with the patterns measured for the symmetrical geometry does not reveal significant aberrations such as excessively high sidelobes or beam broadening.

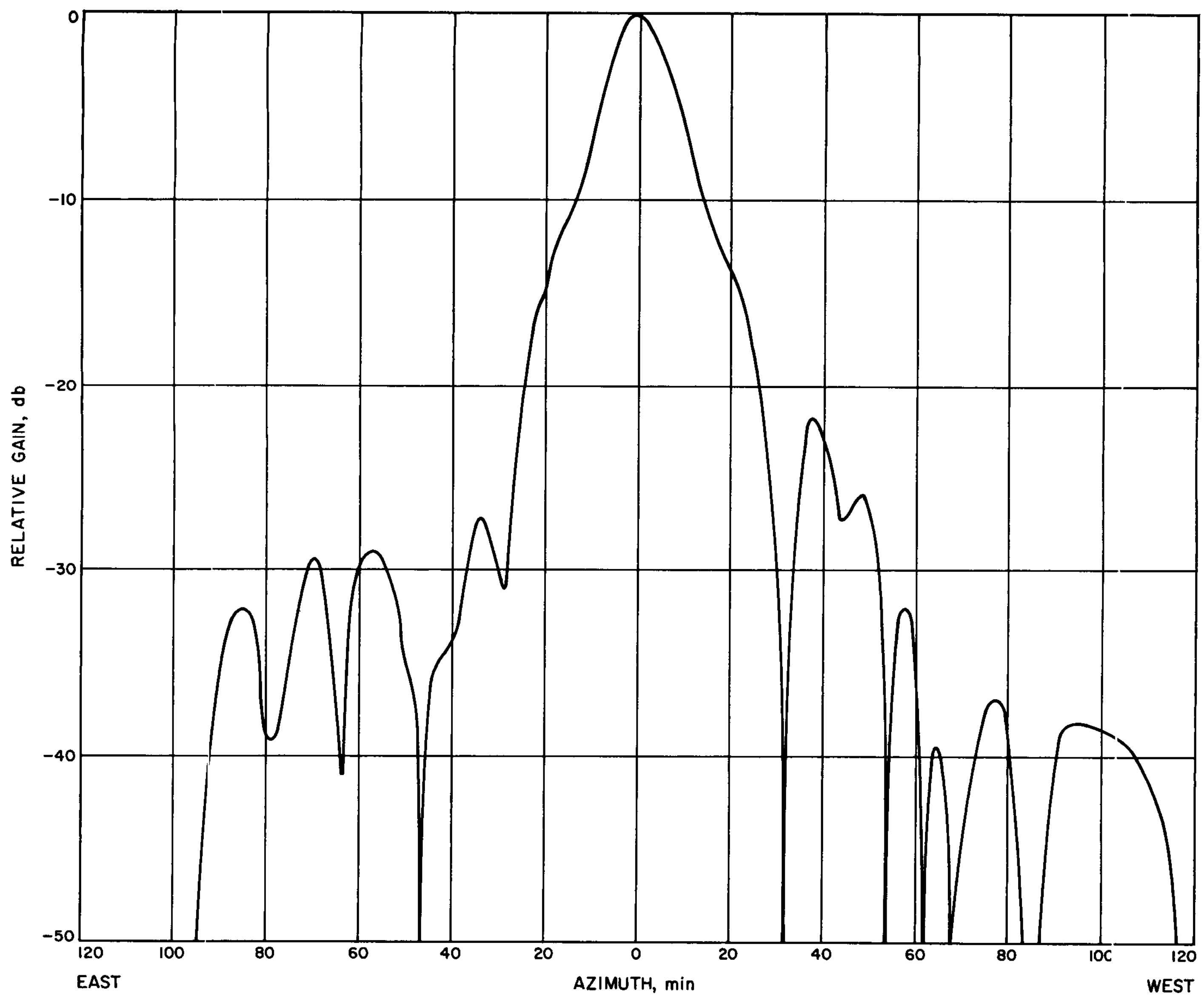

Figure 11 - Azimuth Antenna Pattern

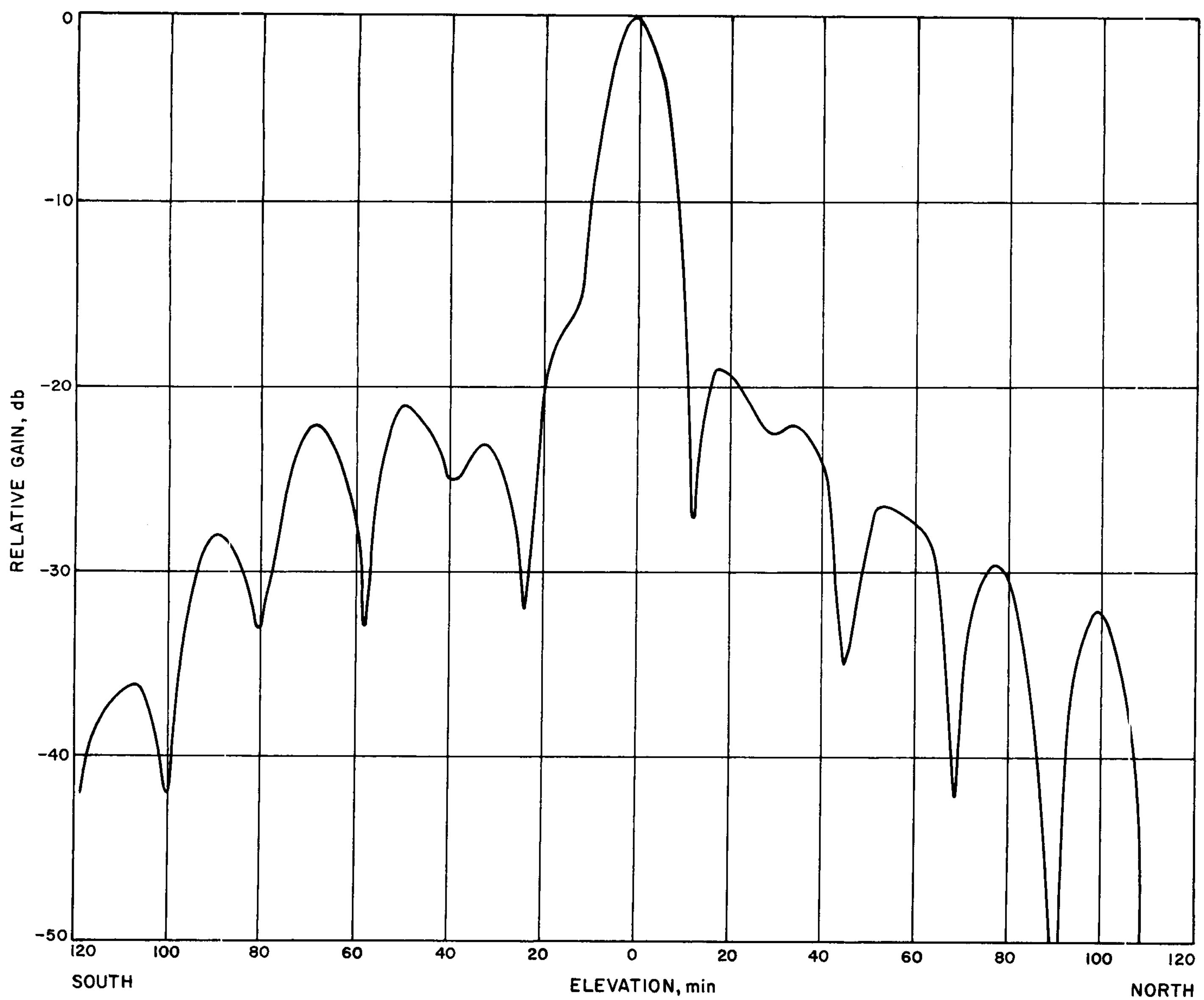

Figure 12 - Elevation Antenna Pattern

IV. SOLAR OBSERVATIONS

Sixteen 3.3 mm observations of the sun were carried out on February 8, 1966. The observational technique was identical to past observational techniques (Ref. 1). Eight observations prior to meridian transit yielded $T'_S / T_{GT} = 3.07 \pm .16$ (p.e.), where T'_S is the equivalent blackbody antenna disc temperature of the sun and T_{GT} was the equivalent excess noise temperature of the gas tube at the output of the waveguide switch. The eight observations following meridian transit yielded $T'_S / T_{GT} = 3.16 \pm .03$ (p.e.). Averaging these two values (to allow for the possibility of a uniform rate of change of atmospheric loss) yielded $T'_S / T_{GT} = 3.12 \pm .08$ (p.e.). Calibration of the equivalent excess noise temperature of the gas tube at the output of the waveguide switch yielded $T_{GT} \doteq 1181.3 \pm 11.4$ °K. (The gas tube output passed through a 10-db directional coupler into the main rf path.) This result then yielded $T'_S = 3683.2 \pm 100.9$ °K. The equivalent blackbody disc temperature of the sun, T_S, is then obtained by dividing T'_S by the beam correction factor (BCF) which was measured to be 0.58 for a solar radius of 16'15''. The final result of this measurement was $T_S = 6378.97 \pm 174.7$ °K.

During the eight post-transit observations on February 8, the observations were also calibrated directly with the hot reference loads that were used to calibrate the gas tube, which served as a transfer standard. The results of this calibration technique yielded $T_S = 6277.6 \pm 230.7$ °K.

Following the observations of February 8, the Tucor, Inc. gas tube was replaced with an ITT, Inc. gas tube. It was expected that the new gas tube would provide more stability in the magnitude of the calibration pulses. Then on five days (February 12, 16, 17, 18, 19) pre- and post-transit observations were made. A typical set of data is plotted in Figure 13. Averaging and reduction of the data taken on these five days yielded:

Date	T_S (°K)	P. E. (°K)
February 12	6372.7	89.5
February 16	6655.3	46.8
February 17	6272.0	41.9
February 18	6190.2	54.0
February 19	6331.2	90.6

The average of these five values, weighted inversely as the probable error, is $T_S = 6375.1 \pm 61.6\ ^{o}K$. This value is not far from the 3.2 mm value of 6402 °K (Ref. 6). It should be noted that the probable error quoted is statistical only. It does not include the large uncertainty involved in the determination of the BCF which brings an additional uncertainty of 7 - 9 %.

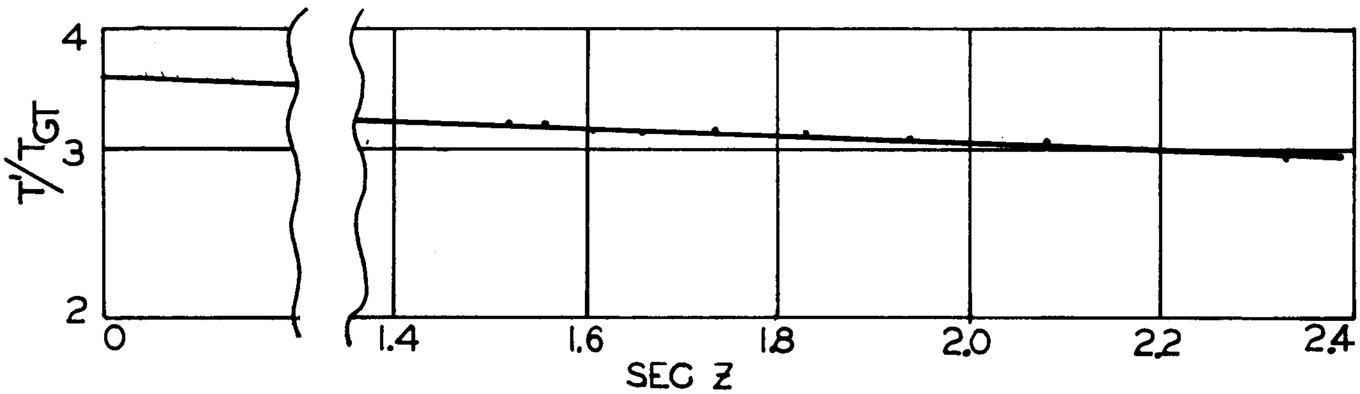

Figure 13 - 16 February 1966 Solar Data (0857 - 1104 PST) with "Best-fit" Straight Line Approximation
$T'_S / T_{GT} = 3.585 \pm 0.022$ (p. e.); $L_o = 1.083 \pm 0.004$ (p. e.)

V. LUNATION OBSERVATIONS

A series of lunation observations was carried out from the period 4 April to 10 July. Useful data was obtained on only 23 dates in this period, due to bad weather and a frequent lack of observing personnel. The observing technique is similar to that used for a similar experiment (Ref. 1). Calibration procedures were carried out each day, using both an ITT, Inc. and a Tucor, Inc. gas tube. The calibration technique is also described in Ref. 1.

Since it was necessary to obtain a Beam Correction Factor in order to convert the antenna temperatures into equivalent blackbody disc temperatures of the moon, it was necessary to remeasure the antenna gain and pattern. A slightly higher gain and somewhat narrower beamwidth were measured than previously.

The resulting lunation curve is plotted in Figure 14. Comparison of this curve with the previous lunation curve (Figure V-9, p. 54, Ref. 1) indicates a reduced scatter of data points as well as a reduced uncertainty for each data point. The increased accuracy was obtained by increasing the period of the on-off cycle and taking more data points. In addition, every data point in Figure 14 is the result of averaging both pre- and post-transit data. The resulting scatter of the data points in Figure 14 is attributed primarily to changing atmospheric loss rather than to experimental uncertainty. It is evident that changes in atmospheric loss during the course of a series of observations can frequently produce misleading data. The process of averaging pre- and post-transit data usually results in smoothing the scatter but does not eliminate it.

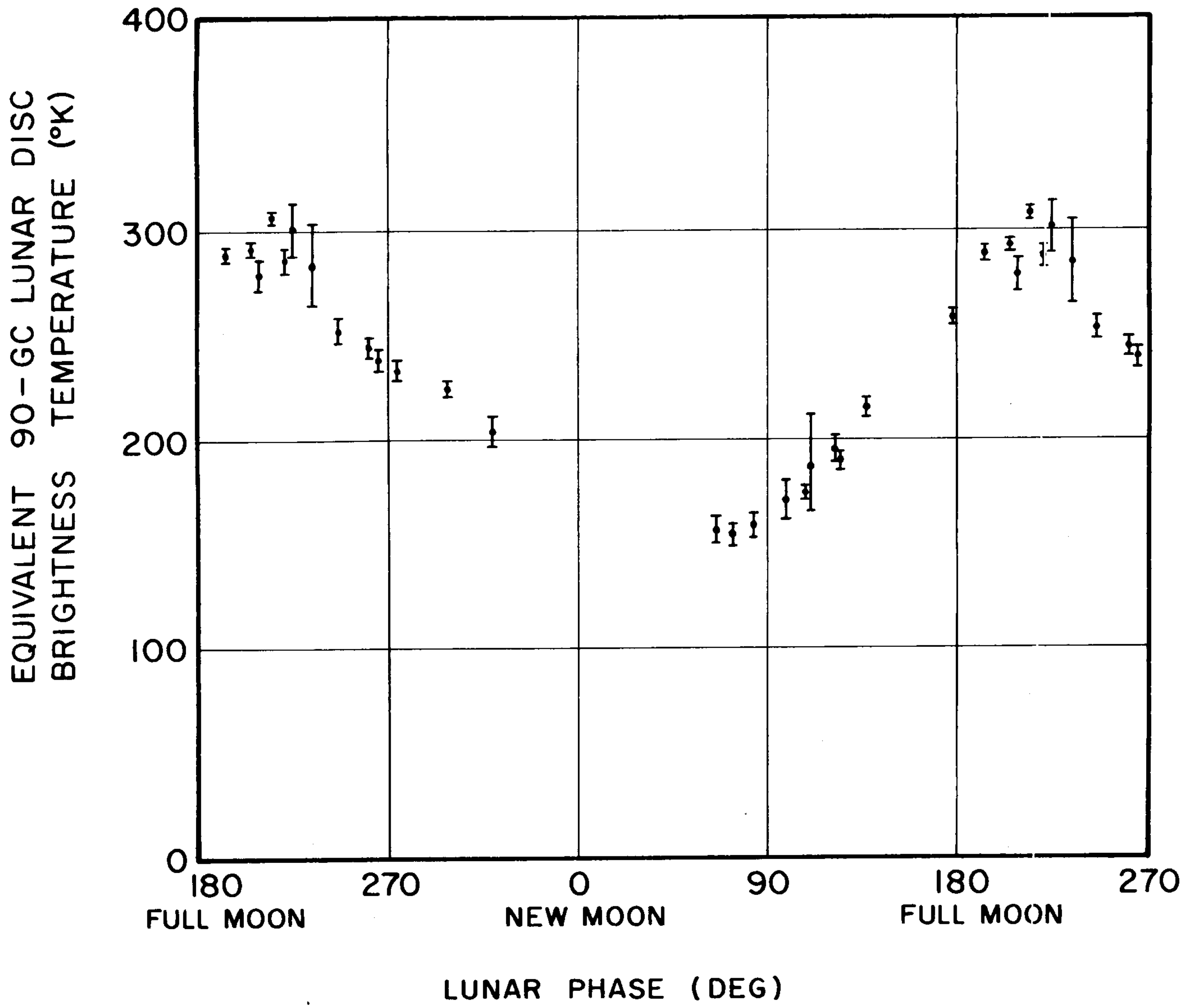

Figure 14 - Lunation Curve (4 April - 10 July 1966)

VI. PUBLICATIONS

1. W. V. T. Rusch and C. T. Stelzried, "Observations of the 19 December 1964 Lunar Eclipse at a Wavelength of 3.3 Millimeters", to be published in the Astrophysical Journal, April 1967.

2. C. T. Stelzried and W. V. T. Rusch, "Improved Determination of Atmospheric Opacity from Radio Astronomy Measurements", to be published in the Journal of Geophysical Research.

APPENDIX

```
      DIMENSION SUM(4),SUMT(4),DATE(12)
    1 READ INPUT TAPE 5,1000,DATE
      READ INPUT TAPE 5,1001,LOOPA,LOOPB,IPRNT
      READ INPUT TAPE 5,1002,THES,DELTHE,THENUM
      READ INPUT TAPE 5,1002,PHIS,DELPHI,PHINUM
      READ INPUT TAPE 5,1002,THEO,CEP,E,ALPHA,CAYX,CAYZ,CAYOF
      LPRNT=0
      LOOPA=(LOOPA/2)*2
      LOOPB=(LOOPB/2)*2
      PI=3.14159265
      PI2=6.2831853
      PIH=1.5707963
      DEG=0.0174532925
      RAD=57.2957795
      WRITE OUTPUT TAPE 6,4000,DATE
      WRITE OUTPUT TAPE 6,5000
      WRITE OUTPUT TAPE 6,5001,THES,DELTHE
      WRITE OUTPUT TAPE 6,5002,PHIS,DELPHI
      WRITE OUTPUT TAPE 6,5003,THEO,CEP,E,ALPHA
      WRITE OUTPUT TAPE 6,5004,CAYX,CAYZ,CAYOF
      ALPHA=ALPHA*DEG
      THES=THES*DEG
      DELTHE=DELTHE*DEG
      PHIS=PHIS*DEG
      THEO=THEO*DEG
      DELPHI=DELPHI*DEG
      DELTH3=(PI-THEO)/FLOATF(LOOPA)
      TEMP=DELTH3*RAD
      WRITE OUTPUT TAPE 6,5005,DELTH3,TEMP
      SINA=SINF(ALPHA)
      COSA=COSF(ALPHA)
      R1=DELTH3/3.0
      JFK=THENUM
      LBJ=PHINUM
      A=LOOPA
      B=LOOPB
      DEL=(B-4.0)/A
      LOOPA=LOOPA+1
      DO 900 L=1,LBJ
      PHI=PHIS+DELPHI*FLOATF(L-1)
      TEMP=PHI*RAD
      WRITE OUTPUT TAPE 6,6000,PHI,TEMP
      WRITE OUTPUT TAPE 6,6001
      WRITE OUTPUT TAPE 6,6002
      SINP=SINF(PHI)
      COSP=COSF(PHI)
      DO 800 K=1,JFK
      THE=THES+DELTHE*FLOATF(K-1)
      SINT=SINF(THE)
      COST=COSF(THE)
      CTCP=COST*COSP
      DO 30 I=1,4
   30 SUMT(I)=0.0
      CTSP=COST*SINP
      IF(IPRNT)34,35,34
   34 LRUN=1
      WRITE OUTPUT TAPE 6,7000,LRUN,SINA,SINP,SINT,CTSP,COSA,COSP,
     XCOST,CTCP,THE,DEL
   35 LL=1
```

```
      DO 600 J=1,LOOPA
      FLOAT=J-1
      THE3=THEO+DELTH3*FLOAT
      NN=B+0.5-DEL*FLOAT
      NN=(NN/2)*2
      DELPH3=PI2/FLOATF(NN)
      R2=DELPH3/3.0
      NN=NN+1
      SINT3=SINF(THE3)
      COST3=COSF(THE3)
      T1=1.0+E*COST3
      CAYRO3=-CEP/T1
      CAYZ3=CAYRO3*COST3
      ECOST3=E+COST3
      SAECT3=SINA*ECOST3
      FTHETA=SINT3/(T1*T1)
      R3=FTHETA*R2
      R4=R3*2.0
      R5=R3*4.0
      DO 40 I=1,4
   40 SUM(I)=0.0
      IF(IPRNT)41,42,41
   41 LRUN=2
      TEMP=DELPH3*RAD
      WRITE OUTPUT TAPE 6,7001,LRUN,THE3,T1,CAYRO3,R3,SINT3,ECOST3,
     XCAYZ3,R4,COST3,SAECT3,FTHETA,R5,DELPH3,TEMP
   42 KK=1
      DO 400 I=1,NN
      PHI3=DELPH3*FLOATF(I-1)
      SINP3=SINF(PHI3)
      COSP3=COSF(PHI3)
      ST3CP3=SINT3*COSP3
      ST3SP3=SINT3*SINP3
      CAYX3=CAYRO3*ST3CP3
      CAYY3=CAYRO3*ST3SP3
      CAYX1=CAYX3*COSA-CAYZ3*SINA-CAYX
      CAYY1=CAYY3
      CAYZ1=CAYX3*SINA+CAYZ3*COSA-CAYZ
      T2=CAYX1**2+CAYY1**2
      CAYRO1=SQRTF(T2+CAYZ1**2)
      T3=SQRTF(T2)
      THE1=PI-ATANF(T3/ABSF(CAYZ1))
      PHI1=ACOSF(ABSF(CAYX1)/T3)
      IF(CAYX1)70,50,50
   50 IF(CAYY1)60,100,100
   60 PHI1=PI2-PHI1
      GO TO 100
   70 IF(CAYY1)80,90,90
   80 PHI1=PI+PHI1
      GO TO 100
   90 PHI1=PI-PHI1
  100 CAYX2=CAYX1
      CAYY2=CAYY1
      CAYZ2=CAYZ1+CAYOF
      CAYRO2=SQRTF(T2+CAYZ2**2)
      IF(CAYZ2)110,130,120
  110 THE2=PI-ATANF(T3/ABSF(CAYZ2))
      GO TO 140
  120 THE2=ATANF(T3/CAYZ2)
```

```
      GO TO 140
  130 THE2=PIH
  140 PHI2=PHI1
      CC=COSA*ST3CP3-SINA*ECOST3
      DD=ST3SP3
      EE=SINA*ST3CP3+COSA*ECOST3
      SINT1=SINF(THE1)
      COST1=COSF(THE1)
      SINP1=SINF(PHI1)
      COSP1=COSF(PHI1)
      FF=(1.0+COST1)*SINP1*COSP1
      GG=COST1*SINP1*SINP1-COSP1*COSP1
      HH=-SINT1*SINP1
      T4=DD*HH-EE*GG
      T5=EE*FF-CC*HH
      T6=CC*GG-DD*FF
      AM=T4*CTCP+T5*CTSP-T6*SINT
      AN=T5*COSP-T4*SINP
      CALL OPTION(THE1,ANS,L)
      AA=ANS
      CALL OPTION(THE1,ANS,L)
      BB=ANS
      T7=CAYRO3/CAYRO1
      G1=T7*AM
      G2=T7*AN
      T8=COSF(PHI-PHI2)
      T9=SINT*SINF(THE2)
      S1=COST*COSF(THE2)
      H=CAYRO2*(T9*T8+S1)-CAYRO1
      SINH=SINF(H)
      COSH=COSF(H)
      S2=AA*COSH-BB*SINH
      S3=BB*COSH+AA*SINH
      IF(I-LOOPB)170,200,170
  170 GO TO(200,220,240),KK
  200 SUM(1)=SUM(1)+G1*S2
      SUM(2)=SUM(2)+G1*S3
      SUM(3)=SUM(3)+G2*S2
      SUM(4)=SUM(4)+G2*S3
      KK=3
      GO TO 300
  220 SUM(1)=SUM(1)+G1*S2*2.0
      SUM(2)=SUM(2)+G1*S3*2.0
      SUM(3)=SUM(3)+G2*S2*2.0
      SUM(4)=SUM(4)+G2*S3*2.0
      KK=3
      GO TO 300
  240 SUM(1)=SUM(1)+G1*S2*4.0
      SUM(2)=SUM(2)+G1*S3*4.0
      SUM(3)=SUM(3)+G2*S2*4.0
      SUM(4)=SUM(4)+G2*S3*4.0
      KK=2
  300 IF(IPRNT)305,400,305
  305 LRUN=3
      WRITE OUTPUT TAPE 6,7002,LRUN,PHI3,THE1,SINT1,CAYX1,SINP3,THE2,
     XCOST1,CAYY1,COSP3,PHI1,SINP1,CAYZ1
      WRITE OUTPUT TAPE 6,7003,ST3CP3,PHI2,COSP1,T2,ST3SP3,CAYX3,
     XCAYY3,T3,T4,T5,T6,T7
      WRITE OUTPUT TAPE 6,7004,T8,T9,S1,S2,S3,CAYX2,CAYRO1,AA,H,
```

```
      XCAYY2,G1,BB
       WRITE OUTPUT TAPE 6,7005,SINH,CAYZ2,G2,CC,COSH,AM,AN,
      XDD,EE,FF,GG,HH,CAYRO2
       WRITE OUTPUT TAPE 6,7006,SUM(1),SUM(2),SUM(3),SUM(4),
      XSUMT(1),SUMT(2),SUMT(3),SUMT(4)
       LPRNT=LPRNT+1
       IF(LPRNT-IPRNT)400,400,310
  310  IPRNT=0
  400  CONTINUE
       IF(J-LOOPA)420,440,420
  420  GO TO(440,460,480),LL
  440  SUMT(1)=SUMT(1)+SUM(1)*R3
       SUMT(2)=SUMT(2)+SUM(2)*R3
       SUMT(3)=SUMT(3)+SUM(3)*R3
       SUMT(4)=SUMT(4)+SUM(4)*R3
       LL=3
       GO TO 600
  460  SUMT(1)=SUMT(1)+SUM(1)*R4
       SUMT(2)=SUMT(2)+SUM(2)*R4
       SUMT(3)=SUMT(3)+SUM(3)*R4
       SUMT(4)=SUMT(4)+SUM(4)*R4
       LL=3
       GO TO 600
  480  SUMT(1)=SUMT(1)+SUM(1)*R5
       SUMT(2)=SUMT(2)+SUM(2)*R5
       SUMT(3)=SUMT(3)+SUM(3)*R5
       SUMT(4)=SUMT(4)+SUM(4)*R5
       LL=2
  600  CONTINUE
       DO 650 I=1,4
  650  SUMT(I)=SUMT(I)*R1
       TEMP=THE*RAD
       T1=SQRTF(SUMT(1)**2+SUMT(2)**2)
       T2=SQRTF(SUMT(3)**2+SUMT(4)**2)
       WRITE OUTPUT TAPE 6,6003,THE,TEMP,SUMT(1),SUMT(2),T1,SUMT(3),
      XSUMT(4),T2
  800  CONTINUE
  900  CONTINUE
       GO TO 1
 1000  FORMAT(12A6)
 1001  FORMAT(14I5)
 1002  FORMAT(7F10.0)
 4000  FORMAT(1H1,30X,12A6)
 5000  FORMAT(39H0INPUT PARAMETERS AND CONTROL CONSTANTS)
 5001  FORMAT(7H0THETA=F12.5,8H DEGREES,10X,10HINCREMENT=F12.5)
 5002  FORMAT(5H PHI=F12.5,8H DEGREES,12X,10HINCREMENT=F12.5)
 5003  FORMAT(10H0THETA(0)=F12.5,10X,3HKEP,6X,1H=,F12.5,10X,1HE,8X,1H=,
      XF12.5,10X,10HALPHA     =F12.5)
 5004  FORMAT(3H KX,6X,1H=F12.5,10X,2HKZ,7X,1H=F12.5,10X,3HKOF,6X,
      X1H=F12.5)
 5005  FORMAT(21H0OUTER INTEGRAL STEP=F12.5,10H RADIANS =F12.5,8H DEGREES
      X)
 6000  FORMAT(5H1PHI=F12.5,9H RADIANS=F12.5,8H DEGREES)
 6001  FORMAT(1H0,13X,5HTHETA,31X,7HE THETA,40X,5HE PHI)
 6002  FORMAT(1H0,5X,7HRADIANS,8X,7HDEGREES,11X,4HREAL,6X,9HIMAGINARY,6X,
      X9HMAGNITUDE,11X,4HREAL,6X,9HIMAGINARY,6X,9HMAGNITUDE/1H )
 6003  FORMAT(8F15.8)
 7000  FORMAT(1H0,I2,4X,7HSINA   =F15.8,8X,7HSINP   =F15.8,8X,7HSINT   =F15.
      X8,8X,7HCTSP   =F15.8/7X,7HCOSA   =F15.8,8X,7HCOSP   =F15.8,8X,7HCOST
```

```
    X =F15.8,8X,7HCTCP   =F15.8/7X,7HTHE    =F15.8,8X,7HDEL    =F15.8)
7001 FORMAT(1H0,I2,4X,7HTHE3   =F15.8,8X,7HT1     =F15.8,8X,7HCAYR03=F15.
    X8,8X,7HR3     =F15.8/7X,7HSINT3 =F15.8,8X,7HECOST3=F15.8,8X,7HCAYZ3
    X =F15.8,8X,7HR4     =F15.8/7X,7HCOST3 =F15.8,8X,7HSAECT3=F15.8,8X,
    X7HFTHETA=F15.8,8X,7HR5      =F15.8/7X,7HDELPH3=F15.8,8X,7HIN DEG=F15
    X.8)
7002 FORMAT(1H0,I2,4X,7HPHI3   =F15.8,8X,7HTHE1   =F15.8,8X,7HSINT1 =F15.
    X8,8X,7HCAYX1 =F15.8/7X,7HSINP3 =F15.8,8X,7HTHE2   =F15.8,8X,7HCOST1
    X =F15.8,8X,7HCAYY1 =F15.8/7X,7HCOSP3 =F15.8,8X,7HPHI1   =F15.8,8X,
    X7HSINP1 =F15.8,8X,7HCAYZ1 =F15.8)
7003 FORMAT(7X,7HST3CP3=F15.8,8X,7HPHI2   =F15.8,8X,7HCOSP1 =F15.8,8X,7H
    XT2     =F15.8/7X,7HST3SP3=F15.8,8X,7HCAYX3 =F15.8,8X,7HCAYY3 =F15.8
    X,8X,7HT3     =F15.8/7X,7HT4     =F15.8,8X,7HT5     =F15.8,8X,7HT6
    X=F15.8,8X,7HT7     =F15.8)
7004 FORMAT(7X,7HT8     =F15.8,8X,7HT9     =F15.8,8X,7HS1     =F15.8,8X,7H
    XS2     =F15.8/7X,7HS3     =F15.8,8X,7HCAYX2 =F15.8,8X,7HCAYR01=F15.8
    X,8X,7HAA     =F15.8/7X,7HH      =F15.8,8X,7HCAYY2 =F15.8,8X,7HG1
    X=F15.8,8X,7HBB     =F15.8)
7005 FORMAT(7X,7HSINH   =F15.8,8X,7HCAYZ2 =F15.8,8X,7HG2     =F15.8,8X,7H
    XCC     =F15.8/7X,7HCOSH   =F15.8,8X,7HAM     =F15.8,8X,7HAN     =F15.8
    X,8X,7HDD     =F15.8/7X,7HEE     =F15.8,8X,7HFF     =F15.8,8X,7HGG
    X=F15.8,8X,7HHH     =F15.8/7X,7HCAYR02=F15.8)
7006 FORMAT(7X,7HSUM   1=F15.8,8X,7HSUM   2=F15.8,8X,7HSUM   3=F15.8,8X,7H
    XSUM   4=F15.8/7X,7HSUMT 1=F15.8,8X,7HSUMT 2=F15.8,8X,7HSUMT 3=F15.8
    X,8X,7HSUMT 4=F15.8)
     END
     SUBROUTINE OPTION(X,Y,L)
     Y=0.0
     IF(X-3.14159265)10,10,30
  10 IF(X-2.966889)30,20,20
  20 Y=1.0
  30 RETURN
     END
```

REFERENCES

1. W. V. T. Rusch, S. Slobin, and C.T. Stelzried, "Millimeter-Wave Radiometry for Radio Astronomy", USCEE Report 161, Electronics Sciences Laboratory, Univ. of So. Calif., Los Angeles, Calif.

2. P. D. Potter, "A New Horn Antenna with Suppressed Sidelobes and Equal Beamwidths", The Microwave Journal, Vol. VI, No. 6, pp. 71-78, June 1963.

3. A. W. Love, "The Diagonal Horn Antenna", The Microwave Journal, Vol. V, No. 3, pp. 117-122, March 1962.

4. S. Silver, "Microwave Antenna Theory and Design", M.I.T. Radiation Lab Series, McGraw-Hill Book Co., Inc., New York, N.Y., Vol. 12, p. 149, 1949.

5. M. P. S. Grønlund, J. Wested, and N. Vejgaard-Nielsen, "Nutating Subreflector in a Cassegrainian Antenna System", Microwave Laboratory, Danish Academy of Technical Sciences, Copenhagen, Denmark, March 1, 1966.

6. M. Simon, "Solar Observations at 3.2 mm", CSUAC 10, Cornell-Sydney University Astronomy Center, Cornell University, Ithaca, New York, November 1964.

ACKNOWLEDGEMENT

We wish to acknowledge several individuals who have participated in this program. Mr. Robert Gardner of JPL continued his excellent work of radiometer development and equipment maintenance during the past year. Mr. Anthony Giandomenico was primarily responsible for the mechanical design of the nodding subdish mechanism and assisted in the initial mechanical testing. Mr. Louis Combe of the Skarda Manufacturing Company was primarily responsible for the fabrication of the nodding subdish. His original innovations during the construction phase contributed invaluably to the project. He is also responsible for the fabrication of the diagonal feedhorn. Mr. M. Dooley, Mr. A. Cooper, Mr. P. Janca, Mr. D. Oltmans, Mr. D. Lynn, and Mr. R. Kellogg of USC assisted in the lunar and solar observation programs. Mr. Palmer Poulson developed the computer program concerning scattering from the tilted hyperboloid.